

Crystal structure and powder X-ray diffraction data of the super-paramagnetic compound CuFeInTe_3

G. E. Delgado^{a,f,*}, P. Grima-Gallardo^{b,c}, J. A. Aitken^d, H. Cabrera^e, J. Cisterna^f, A. Cárdenas^g, and I. Brito^f

^aLaboratorio de Cristalografía, Departamento de Química, Facultad de Ciencias, Universidad de Los Andes, Mérida, 5101, Venezuela.

*e-mail: gerzon@ula.ve

^bCentro de Estudios de Semiconductores, Departamento de Física, Facultad de Ciencias, Universidad de Los Andes, Mérida 5101, Venezuela.

^cCentro Nacional de Tecnologías Ópticas y Centro Investigaciones de Astronomía, Mérida 5101, Venezuela.

^dDepartment of Chemistry and Biochemistry, Duquesne University, Pittsburgh, Pennsylvania 15282, United States.

^eSezione di Trieste, Istituto Nazionale di Fisica Nucleare, 34149 Trieste, Italy.

^fDepartamento de Química, Facultad de Ciencias Básicas, Universidad de Antofagasta, Avda. Universidad de Antofagasta 02800, Campus Coloso, Antofagasta, 1240000, Chile.

^gDepartamento de Física, Facultad de Ciencias Básicas, Universidad de Antofagasta, Avda. Universidad de Antofagasta 02800, Campus Coloso, Antofagasta, 1240000, Chile.

Received 7 November 2020; accepted 29 November 2020

The crystal structure of the new CuFeInTe_3 quaternary compound was studied by the Rietveld method from powder X-ray diffraction data. The CuFeInTe_3 compound crystallize in the tetragonal CuFeInTe_3 -type structure with space group $P\bar{4}2c$ ($N^\circ 112$), and unit cell parameters $a = 6.1842(1) \text{ \AA}$, $c = 12.4163(2) \text{ \AA}$, $V = 474.85(1) \text{ \AA}^3$. The density of CuFeInTe_3 is $\rho_x = 5.753 \text{ g cm}^{-3}$. The reliability factors of the Rietveld refinement results are $R_p = 5.5\%$, $R_{wp} = 6.1\%$, $R_{exp} = 4.7\%$, and $S = 1.3$. The powder XRD data of CuFeInTe_3 are presented and the figures of merit of indexation are $M_{20} = 79.4$ and $F_{30} = 43.3$ (0.0045, 154).

Keywords: Crystal structure; powder X-ray diffraction data; Rietveld; chalcogenide; semiconductor; alloys.

PACS: 61.05.cp; 61.50.Nw; 61.66.Fn; 61.40.b

DOI: <https://doi.org/10.31349/RevMexFis.67.305>

1. Introduction

CuInTe_2 is a well-known semiconductor of the I-III-VI₂ family, which crystallizes in a chalcopyrite structure, space group I 2d ($N^\circ 121$), with unit cell parameters $a = 6.194(2) \text{ \AA}$ and $c = 12.416(4) \text{ \AA}$ [1,2]. Recently, attention has been focused to explore their potential application in thermoelectric technology due to their moderate electrical transports and low thermal conductivity. A dimensionless figure of merit $zT (= \alpha^2 \sigma T / \kappa$, where α , σ , T , and κ are Seebeck coefficient, electrical conductivity, absolute temperature, and thermal conductivity, respectively) of 1.18 at 850 K has been reported, which is better than any other un-doped diamond-like material [3]. To enhance the figure of merit, CuInTe_2 can be doped or alloyed; throughout these procedures, it is possible to tune the carrier concentration optimizing both electrical conductivity (σ) and power factor ($\alpha^2 \sigma$) and also to create extrinsic defects which could greatly alter the electron and phonon transport properties. It has been reported [4] that when CuInTe_2 is doped with Cd according with the general expression $\text{CuIn}_{1-x}\text{Cd}_x\text{Te}_2$ (with $x = 0, 0.02, 0.05$, and 0.1) the zT values were improved by over 100% at room temperature and around 20% at 600 K for $x = 0.02$ and 0.1 , respectively. It had been also reported [5] that $(\text{CuInTe}_2)_{1-x}(\text{ZnTe})_x$ solid solutions (simultaneous Zn^{2+}

substitution for both Cu^+ and In^{3+}) have a lower thermal conductivity than CuInTe_2 and attained $zT = 0.69$ at 737 K, which is 1.65 times higher than the zT value of Zn-free CuInTe_2 .

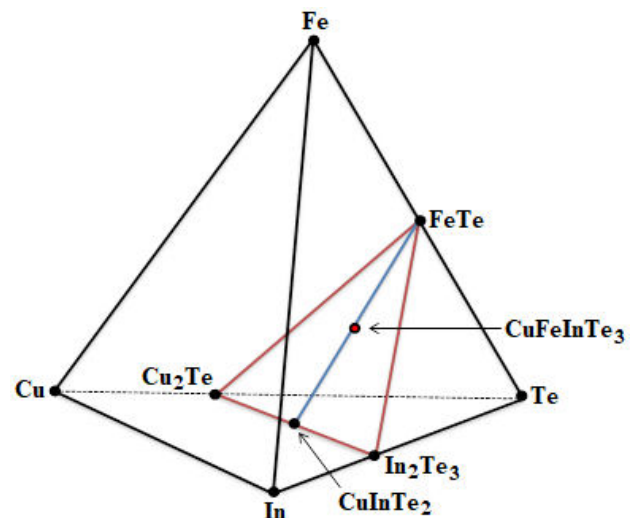


FIGURE 1. Compositional representation of the Cu-Fe-In-Te quaternary solid solutions system.

TABLE I. X-ray powder diffraction data of the quaternary CuFeInTe₃.

$2\theta_{\text{obs}}(^{\circ})$	$d_{\text{obs}}(\text{\AA})$	$(I/I_0)_{\text{obs}}$	h	k	l	$2\theta_{\text{cal}}(^{\circ})$	$d_{\text{cal}}(\text{\AA})$	$\Delta 2\theta(^{\circ})$
16.001	5.5341	1.0	1	0	1	15.994	5.5367	-0.007
24.896	3.5734	100.0	1	1	2	24.889	3.5743	-0.007
25.920	3.4345	3.1	1	0	3	25.915	3.4352	-0.005
28.829	3.0942	1.9	2	0	0	28.826	3.0945	-0.003
			0	0	4	28.800	3.0973	
33.141	2.7008	6.4	2	1	1	33.135	2.7013	-0.006
			1	0	5	39.126	2.3003	
39.143	2.2994	1.6	2	1	3	39.146	2.2992	0.003
41.199	2.1892	47.0	2	0	4	41.201	2.1891	0.002
41.222	2.1881	30.8	2	2	0	41.220	2.1882	-0.002
44.487	2.0348	2.6	3	0	1	44.482	2.0350	-0.005
			1	1	6	48.720	1.8674	
48.755	1.8662	26.0	3	1	2	48.753	1.8662	-0.002
53.819	1.7019	0.9	1	0	7	53.828	1.7016	0.009
			3	2	1	53.874	1.7003	
55.509	1.6540	0.8	3	2	2	55.502	1.6542	-0.007
58.136	1.5854	1.9	3	0	5	58.134	1.5854	-0.002
			3	2	3	58.148	1.5851	
59.650	1.5487	2.5	0	0	8	59.653	1.5486	0.003
59.712	1.5472	4.1	4	0	0	59.711	1.5473	-0.001
			2	1	7	62.205	1.4911	
62.239	1.4904	0.9	0	4	1	62.247	1.4902	0.008
			3	1	6	65.674	1.4205	
65.704	1.4199	8.4	3	3	2	65.702	1.4199	-0.002
66.161	1.4112	1.7	3	2	5	66.170	1.4110	0.009
			4	1	3	66.183	1.4108	
67.589	1.3848	0.7	2	0	8	67.584	1.3849	-0.005
			4	0	4	67.624	1.3842	
73.732	1.2839	0.7	4	1	5	73.733	1.2839	0.001
75.078	1.2642	9.4	2	2	8	75.083	1.2641	0.005
			4	2	4	75.122	1.2635	
77.379	1.2322	0.9	3	2	7	77.379	1.2322	0.000
			4	3	1	77.418	1.2317	
80.509	1.1920	2.9	1	1	10	80.504	1.1921	-0.005
			3	3	6	80.555	1.1914	
81.017	1.1858	0.7	4	3	3	81.025	1.1857	0.008
82.786	1.1649	0.7	4	0	7	82.787	1.1649	0.001
			5	1	3	82.818	1.1645	
84.551	1.1450	0.8	3	0	9	84.548	1.1451	-0.003
			4	1	7	84.573	1.1448	
88.075	1.1081	0.8	1	0	11	88.074	1.1081	-0.001
89.441	1.0947		4	0	8	89.450	1.0946	0.009
			4	4	0	89.500	1.0941	
94.749	1.0468	2.0	3	1	10	94.752	1.0468	0.003
			5	1	6	94.802	1.0464	
98.780	1.0146	0.7	4	1	9	98.789	1.0145	0.009
			4	3	7	98.814	1.0144	

TABLE II. Rietveld refinement results for CuFeInTe₃.

Molecular formula	CuFeInTe ₃	Wavelength (CuK α) (Å)	1.5418
Molecular weight (g/mol)	386.66	Range 2 θ (°)	10-140
a (Å)	6.1842(1)	Step size (°)	0.008
c (Å)	12.4163(2)	Counting Time (s)	40
V (Å ³)	474.85(1)	N°intensities	4501
$\eta = c/2a$	2.01	Independent reflections	322
System	tetragonal	R_{exp} (%)	4.7
Space group	$P\bar{4}2c$	(N°112) R_p (%)	5.5
Z	8/3	R_{wp} (%)	6.1
ρx (g cm ⁻³)	5.753	S	1.3

Following this reasoning, the (CuInTe₂)_{1-x}(ZnTe)_x solid solutions system has been investigated, and more particularly the sample CuFeInTe₃, which corresponds to the value of $x = 0.5$ (see Fig. 1). This quaternary compound is a semiconductor, belonging to the I-II-III-VI₃ family, which has been studied for spintronic applications with interesting magnetic, thermal and thermoelectric properties. Grima-Gallardo *et al.* suggest a super-paramagnetism behavior for CuFeInTe₃ [6,7] and Cabrera *et al.* [8] have demonstrated that CuFeInTe₃ is a promising n -type thermoelectric material applicable at high temperatures.

For this compound, there are no reports on its powder diffraction pattern or its crystalline structure in the appropriate databases reviewed: Powder Diffraction File [9], Inorganic Crystal Structure Database (ICSD) [10], and Springer Materials [11]. Hence, here we present the structural characterization of the quaternary compound CuFeInTe₃ using the Rietveld method to establish its crystal structure and report its powder X-ray diffraction data. The chemical structure was validated using the Bond Valence Sum (BVS) calculations [12,13].

2. Experimental

2.1. Synthesis

The chemical elements Cu, Fe, In, and Te (99.99% of purity, GoodFellow) in stoichiometric quantities, were introduced into a synthetic silica glass ampoule and sealed under vacuum ($\sim 10^{-4}$ Torr). This ampoule was subjected to pyrolysis to avoid reaction of the starting materials with silica glass. The mixture was slowly heated up to 1500 K at a rate of 20 K/h, with a stop of 48 h at 722.5 K (melting temperature of Te) to maximize the formation of binary species at low temperature and minimize the presence of unreacted Te at high temperatures. To ensure complete mixing of all elements, the ampule was kept under constant stirring. At the maximum temperature (1500 K) the ampoule was kept for 48 h and it starts cooling at a rate of 20 K/h, until 873 K which was kept for 30 days. Finally, it was cooled to room temperature at a rate of 10 K/h. The color of the obtained ingots was bright gray and seemed to be homogeneous.

2.2. Powder X-ray diffraction

The specimen of CuFeInTe₃ for XRD measurements was ground in an agate mortar and pestle to a particle size of fewer than 106 μm . Powder X-ray diffraction pattern was collected at room temperature (298 K) on a PANalytical X'Pert Pro MPD powder X-ray diffractometer operating in Bragg-Brentano geometry using CuK α radiation ($\lambda = 1.5418$ Å). A tube power of 45 kV and 40 mA was employed. A nickel filter was used in the diffracted beam optics and the data were collected with the X'Celerator one-dimensional silicon strip detector. A 1/4° divergent slit, a 1/2° anti-scatter slit, and a 0.02 rad soller slit were set at both the incident and diffracted beams. The scan range was from 10 to 140° 2 θ with a step size of 0.008° and a scan speed of 0.0106°/s. The analytical software package Highscore Plus (PANalytical, Almelo, Netherlands) was used to establish the positions of the peaks from the α_1 component, strip mathematically the α_2 component from each reflection, and to determine the peak intensities of the diffraction peaks (Table I). For the Rietveld refinement, the whole diffraction data was used.

3. Results and discussion

The experimental (Yobs in red) powder XRD pattern of CuFeInTe₃ is shown in Fig. 2. An automatic search in the PDF-ICDD database [9], using the software available with the diffractometer, indicated that the powder pattern contained small amounts of Fe_{1.125}Te (PDF N°01-080-0280). Bragg positions of the diffraction lines from this compound are also indicated in Fig. 2. The 20 first peak positions of the main phase, CuFeInTe₃, were successfully indexed using the Dicvol04 program [14], in a tetragonal unit cell with parameters slightly shorter than those of the ternary chalcopyrite parent CuInTe₂ [2].

A space group search using ExtSym program [15] suggested the space group $P\bar{4}2c$ which is consistent with the systematic absences.

The complete powder diffraction dataset was reviewed in the tetragonal space group $P\bar{4}2c$ by using the program

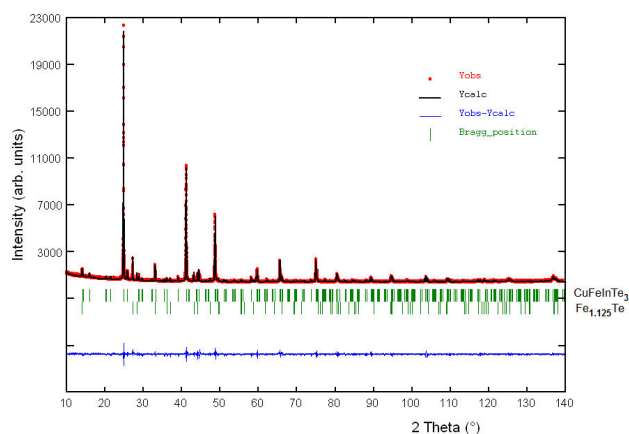


FIGURE 2. Rietveld refinement final plot of CuFeInTe_3 . The lower trace is the difference curve between observed and calculated patterns. The Bragg reflections are indicated by vertical bars.

NBS*AIDS [16]. From this analysis, the refined unit-cell parameters obtained were: $a = 6.1891(3) \text{ \AA}$ and $c = 12.3891(6) \text{ \AA}$, with figures of merit $M_{20} = 79.4$ [17] and $F_{30} = 43.3$ (0.0045, 154) [18]. The resulting powder X-ray diffraction data for CuFeInTe_3 , together with the observed and calculated 2θ , the d-spacing's as well as the relative intensities of the reflections, are given in Table I. These data will be submitted to the Powder Diffraction File of the International Centre for Diffraction Data [9].

The Rietveld refinement technique [19] with the software Fullprof version 7.30, March 2020 [20] was used to determine the structure of CuFeInTe_3 .

The starting structure model used was that of the parent compound CuFeInSe_3 [21] and the unit cell parameters were those obtained from the NBS*AIDS refinement. Atomic positions of the $\text{Fe}_{1.125}\text{Te}$ binary [22] were included as a secondary phase in the refinement. The peak profiles were described using a parametrized pseudo-Voigt function [23,24]. The background was described by the automatic interpolation of 123 points throughout the whole pattern. With the diffrac-

tion data available it was only possible to describe the thermal motion of the atoms by one overall isotropic temperature factor. A total of 23 parameters of the CuFeInTe_3 compound were refined, including peak shape parameters, scale factor, cell parameters, atomic coordinates, isotropic displacement parameters, and full-width at half-maximum (FWHM) parameters. The final Rietveld refinement led to agreement factors of: $R_{\text{exp}} = 4.7\%$, $R_p = 5.5\%$, $R_{\text{wp}} = 6.1\%$, and $S = 1.3$, respectively ($R_{\text{exp}} = 100[(N - P + C) / \sum_w (y_{\text{obs}}^2)]^{1/2}$, $R_p = 100 \sum_w |y_{\text{obs}} - y_{\text{calc}}| / \sum_w |y_{\text{obs}}|$, $R_{\text{wp}} = 100[\sum_w |y_{\text{obs}} - y_{\text{calc}}| / \sum_w |y_{\text{obs}}|^2]^{1/2}$, $S = [R_{\text{wp}} / R_{\text{exp}}]$, $N - P + C$ is the number of degrees of freedom).

Figure 2 shows the results of the Rietveld refinement of CuFeInTe_3 . The calculated powder pattern is shown as a solid black color line. The solid blue line is the difference between the calculated and experimental powder XRD patterns. The vertical green lines show expected Bragg diffraction peaks calculated as per space group $P42c$. Details of refinement values are summarized in Table II. A semi-quantitative analysis [25] from the final Rietveld refinement converged to the weight fraction percentages: CuFeInTe_3 (91.9%) and $\text{Fe}_{1.125}\text{Te}$ (8.1%). Table III shows the atomic coordinates, thermal displacement factors, bond distances, and angles for CuFeInTe_3 . Unit cell diagram for this quaternary compound is shown in Fig. 3.

In this system $(\text{CuInTe}_2)_{1-x}(\text{ZnTe})_x$, with composition $x = 0.5$, introducing an additional cation (Fe) to the ternary CuInTe_2 leads to symmetry reduction from the chalcopyrite structure $I42d$ to a related $P42c$ known as P-chalcopyrite [26]. In Fig. 3 it is possible to observe a comparison, with the tetrahedra pointed in the same direction, between the two structures: the ordered chalcopyrite $I42d$ structure of CuInTe_2 and the partially disordered $P42c$ structure of CuFeInTe_3 . The quaternary compound CuFeInTe_3 has a normal adamantane-structure and can be described as a derivative of the sphalerite structure [27]. The main features in the

TABLE III. Atomic coordinates, isotropic temperature factor, and selected geometric parameters (\AA , $^\circ$) for CuFeInTe_3 , derived from the Rietveld refinement. Bond valence sum (BVS) results are shown, $M = (1/3\text{Cu} + 1/3\text{Fe} + 1/3\text{In})$.

Atom	Ox.	BVS	Wyck.	x	y	z	foc	B (\AA^2)
Cu	+1	1.37	2c	0	1/2	1/4	1	0.35(2)
Fe	+2	2.35	2e	0	0	0	1	0.35(2)
In	+3	3.43	2b	1/2	0	1/4	1	0.35(2)
M		2f		1/2	1/2	1/2	1	0.35(2)
Te	-2	2.37	8n	0.2534(1)	0.2563(1)	0.1176(1)	1	0.35(2)
Cu - Te		2.665(1)	Fe - Te		2.726(1)	In - Te ⁱ		2.746(1)
Te ⁱⁱ - Cu - Te ⁱⁱⁱ		107.8(1) x4	Te - Fe - Te ^v		111.0(1) x4	Te ⁱ - In - Te ^{vii}		110.6(1) x4
Te ⁱⁱ - Cu - Te ^{iv}		112.8(1) x2	Te - Fe - Te ^{vi}		105.7(1) x2	Te ⁱ - In - Te ^{viii}		106.5(1) x2

Symmetry codes: (i) 0.5-x, 0.5-y, 0.5+z; (ii) y, x, z; (iii) 0.5-x, 0.5+y, 0.5-z; (iv) -y, 1-x, z; (v) -x, -y, z; (vi) y, -x, -z; (vii) 0.5-y, -0.5+x, 0.5-z; (viii) -0.5+x, -0.5+y, 0.5+z.

Bond valence sum (BVS): $V_{ij} = \sum_j \exp([R_o - R_{ij}]/b)$, $b = 0.37 \text{ \AA}$, $r_o(\text{Cu-Te}) = 2.27 \text{ \AA}$, $r_o(\text{Fe-Te}) = 2.53 \text{ \AA}$, $r_o(\text{In-Te}) = 2.69 \text{ \AA}$.

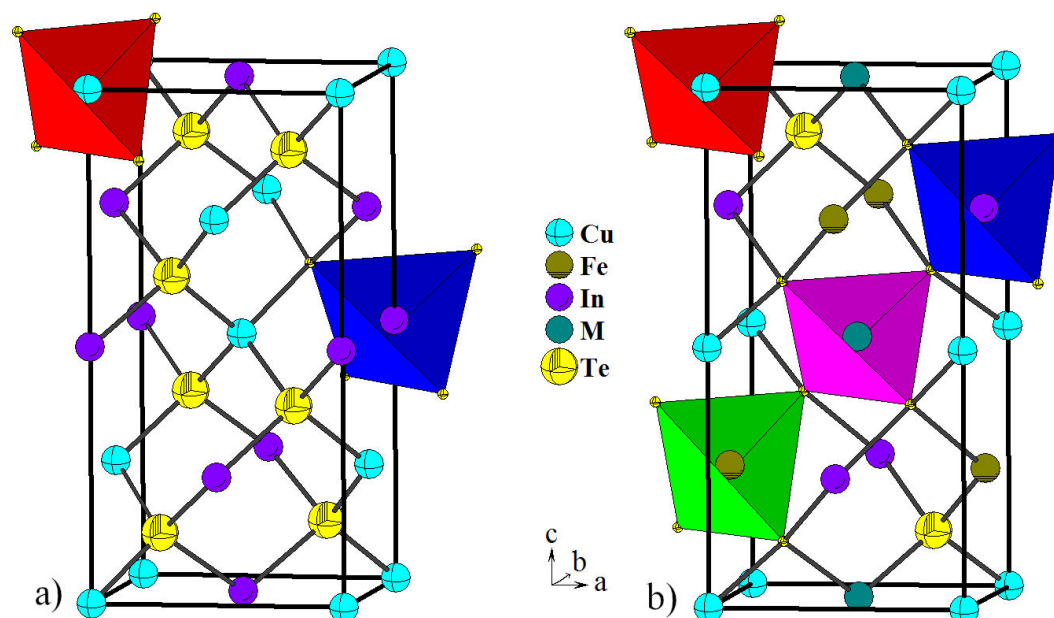


FIGURE 3. Unit cell diagram of the ternary CuInTe_2 ($\bar{I}42d$) chalcopyrite structure a) and the quaternary CuFeInTe_3 ($P\bar{4}2c$) structure, b) showing the tetrahedra around the cations. The two structures differ in the arrangement of cations.

crystal structure are tetrahedral; each cation is coordinated by four anions (Te) and each anion is coordinated by four cations (one Cu, one Fe, one In, and one M) located at the corners of a slightly distorted tetrahedron. The tetrahedra containing the cations atoms have to mean Te...Te distances; 4.279(1) Å for M, 4.456(1) Å for Fe, 4.307(1) Å for Cu, 4.487(1) Å for In, respectively.

The interatomic Cu-Te [2.665(1) Å], Fe-Te [2.726(1) Å], and In-Te [2.746(1) Å] are somewhat smaller than the sum of the respective ionic radii for structures tetrahedrally bonded [28]. However, correlates well with those found in the adamantane structures CuInTe_2 [14], AgIn_5Te_8 [29], $\text{CuTa}_2\text{InTe}_4$ [30], Cu_3NbTe_4 [31], Fe_2GeTe_4 [32], $\text{Ag}_2\text{FeGeTe}_4$ [33], AgInTe_2 [34], $\text{CuCo}_2\text{InTe}_4$ and $\text{CuNi}_2\text{InTe}_4$ [35], $\text{Cu}_3\text{In}_7\text{Te}_{12}$ [36] and $\text{Cu}_3\text{In}_5\text{Te}_9$ [37].

The Bond Valence Sum (BVS) values, for Cu, Fe, In, and Te were calculated using the Brown-Altarmatt empirical expression [11,12]. The BVS of an atom i is defined as the sum of the bond valences V_{ij} of all the bonds from atoms i to atoms j and the usually accepted empirical expression for BVS is $V_{ij} = \exp[(R_o - d_{ij})/B]$, where d_{ij} is the interatomic distance and B is taken to be a "universal" constant equal to 0.37 Å. The values for the reference distance R_o are 2.27 Å, 2.53 Å, and 2.69 Å, for Cu-Te, Fe-Te, and In-Te, respectively [12]. The calculated oxidation states agree with the expected

formal oxidation states for Cu^+ , Fe^{2+} , In^{3+} , and Te^{2-} ions, whose results can also be seen in Table III.

4. Conclusions

The powder X-ray diffraction data and crystal structure of the super-paramagnetic semiconductor CuFeInTe_3 is reported. This compound, refined by the Rietveld method, crystallizes in a P -chalcopyrite structure with a partially disorder cation distribution. Structurally it corresponds to a new adamantane compound and consists of a three-dimensional arrangement of slightly distorted CuTe_4 , FeTe_4 , and InTe_4 tetrahedra connected by common corners. The chemical structural model was checked by analysis of the interatomic distances using the Bond Valence Sum (BVS) formula based on bond-strength examination.

Acknowledgments

This work was partial performed by G.E. Delgado during a visit at the Universidad de Antofagasta, supported by MINEDUC-UA project, code ANT 1856. We thank to CDCHTA-ULA (grant C-1885-14-05-B) and FONACIT (grants LAB-97000821 and 2011001341).

1. J. E. Jaffe and A. Zunger, Theory of the band-gap anomaly in ABC_2 chalcopyrite semiconductors, *Phys. Rev. B* **29** (1984) 1882, <https://doi.org/10.1103/PhysRevB.29.1882>.

2. K. S. Knight, The crystal structures of CuInSe_2 and CuInTe_2 , *Mater. Res. Bull.* **27** (1992) 161, [https://doi.org/10.1016/0025-5408\(92\)90209-I](https://doi.org/10.1016/0025-5408(92)90209-I).

3. R. Liu *et al.*, Ternary compound CuInTe_2 : a promising

- thermoelectric material with diamond-like structure, *Chem. Commun.* **48** (2012) 3818, <https://doi.org/10.1039/C2CC30318C>.
4. N. Cheng *et al.*, Enhanced thermoelectric performance in Cd doped CuInTe₂ compounds, *J. Appl. Phys.* **115** (2014) 163705, <https://doi.org/10.1063/1.4872250>.
 5. J. Yang *et al.*, Lattice defects and thermoelectric properties: the case of p-type CuInTe₂ chalcopyrite on introduction of zinc, *Dalton Trans.* **43** (2014) 15228, <https://doi.org/10.1039/C4DT01909A>.
 6. P. Grima-Gallardo *et al.*, Superparamagnetism in CuFeInTe₃ and CuFeGaTe₃ alloys, *Phys. Status Solidi A* **209** (2012) 1141, <https://doi.org/10.1002/pssa.201127663>.
 7. P. Grima-Gallardo *et al.*, Phase Diagram of (CuInTe₂)_{1-x}(FeTe)_x Alloys (0 ≤ x ≤ 0.6), *Rev. Latinoam. Metal. Mater.* **38** (2018) 53
 8. H. Cabrera *et al.*, Thermoelectric transport properties of CuFeInTe₃, *J. Alloys Compd.* **651** (2015) 490, <https://doi.org/10.1016/j.jallcom.2015.08.128>.
 9. PDF-ICDD, International Centre for Diffraction Data, Newtown Square, USA, 2020.
 10. ICSD, Inorganic Crystal Structure Database, Karlsruhe, Germany, 2016.
 11. Springer Materials, <https://materials.springer.com>, 2020.
 12. I. D. Brown and D. Altermatt, Bond-valence parameters obtained from a systematic analysis of the Inorganic Crystal Structure Database, *Acta Cryst. B* **41** (1985) 244, <https://doi.org/10.1107/S0108768185002063>.
 13. N. E. Brese and M. O'Keeffe, Bond-valence parameters for solids, *Acta Cryst. B* **47** (1991) 192, <https://doi.org/10.1107/S0108768190011041>.
 14. A. Boulfif and D. Louër, Powder pattern indexing with the dichotomy method, *J. Appl. Cryst.* **37** (2004) 724, <https://doi.org/10.1107/S0021889804014876>.
 15. A. J. Markvardsen *et al.*, ExtSym: a program to aid space-group determination from powder diffraction data, *J. Appl. Cryst.* **41** (2008) 1177, <https://doi.org/10.1107/S0021889808031087>.
 16. A. D. Mighell, C. R. Hubbard, J. K. Stalick, NBS*AIDS80, Technical Note 1141, USA, 1981.
 17. P. M. de Wolff, A simplified criterion for the reliability of a powder pattern indexing, *J. Appl. Cryst.* **1** (1968) 108, <https://doi.org/10.1107/S002188986800508X>.
 18. G. S. Smith and R. L. Snyder, *F_N*: A criterion for rating powder diffraction patterns and evaluating the reliability of powder-pattern indexing, *J. Appl. Cryst.* **12** (1979) 60, <https://doi.org/10.1107/S002188987901178X>.
 19. H. M. Rietveld, A profile refinement method for nuclear and magnetic structures, *J. Appl. Cryst.* **2** (1969) 65, <https://doi.org/10.1107/S0021889869006558>.
 20. J. Rodríguez-Carvajal, Recent advances in magnetic structure determination by neutron powder diffraction, *Phys. B* **192** (1993) 55, [https://doi.org/10.1016/0921-4526\(93\)90108-I](https://doi.org/10.1016/0921-4526(93)90108-I).
 21. A. J. Mora, G. E. Delgado, and P. Grima-Gallardo, Crystal structure of CuFeInSe₃ from X-ray powder diffraction data, *Phys. Status Solidi A* **204** (2007) 547, <https://doi.org/10.1002/pssa.200622395>.
 22. D. Fruchart *et al.*, *Mater. Res. Bull.* **10** (1975) 169, [https://doi.org/10.1016/0025-5408\(75\)90151-8](https://doi.org/10.1016/0025-5408(75)90151-8).
 23. G. Caglioti, A. Paoletti, and F. P. Ricci, Choice of collimators for a crystal spectrometer for neutron diffraction, *Nucl. Instrum.* **3** (1958) 223, [https://doi.org/10.1016/0369-643X\(58\)90029-X](https://doi.org/10.1016/0369-643X(58)90029-X).
 24. P. Thompson, D. E. Cox, and J. B. Hastings, Rietveld refinement of Debye-Scherrer synchrotron X-ray data from Al₂O₃, *J. Appl. Cryst.* **20** (1987) 79, <https://doi.org/10.1107/S0021889887087090>.
 25. R. J. Hill and C. J. Howard, Quantitative phase analysis from neutron diffraction data using the Rietveld method, *J. Appl. Cryst.* **20** (1987) 467, <https://doi.org/10.1107/S0021889887086199>.
 26. W. Hönle, G. Kühn, and U.-C. Boehnke, Crystal structures of two quenched Cu-In-Se phases, *Cryst. Res. Technol.* **23** (1988) 1347, <https://doi.org/10.1002/crat.2170231027>.
 27. E. Parthé, *Wurtzite and Sphalerite Structures*, in *Intermetallic Compounds*, edited by J. H. Westbrook and R. L. Fleischer, Vol. 1 (John Wiley and Sons, Chichester, 1995).
 28. R. D. Shannon, Revised effective ionic radii and systematic studies of interatomic distances in halides and chalcogenides, *Acta Cryst. A* **32** (1976) 751, <https://doi.org/10.1107/S0567739476001551>.
 29. A. J. Mora, G. E. Delgado, C. Pineda, and T. Tinoco, Synthesis and structural study of the AgIn₅Te₈ compound by X-ray powder diffraction, *Phys. Status Solidi A* **201** (2004) 1477, <https://doi.org/10.1002/pssa.200406805>.
 30. G. E. Delgado *et al.*, Crystal structure of the quaternary compound CuTa₂InTe₄ from X-ray powder diffraction, *Phys. B* **403** (2008) 3228, <https://doi.org/10.1016/j.physb.2008.04.022>.
 31. G. E. Delgado *et al.*, Synthesis and characterization of the ternary chalcogenide compound Cu₃NbTe₄, *Chalcogenide Lett.* **6** (2009) 335.
 32. G. E. Delgado *et al.*, Synthesis and crystallographic study of the ternary semiconductor compound Fe₂GeTe₄, *Chalcogenide Lett.* **7** (2010) 133.
 33. G. E. Delgado *et al.*, Synthesis and crystal structure of the quaternary compound AgFe₂GaTe₄, *J. Alloys Compd.* **613** (2014) 143, <https://doi.org/10.1016/j.jallcom.2014.06.004>.
 34. G. E. Delgado *et al.*, X-ray powder diffraction data and Rietveld refinement of the ternary semiconductor chalcogenides AgInSe₂ and AgInTe₂, *Rev. Latinoam. Metal. Mater.* **35** (2015) 110.
 35. G. E. Delgado *et al.*, Structural Characterization of Two New Quaternary Chalcogenides: CuCo₂InTe₄ and CuNi₂InTe₄, *Mater. Res.* **19** (2016) 1423, <https://doi.org/10.1590/1980-5373-mr-2016-0098>.

36. G. E. Delgado *et al.*, Evidence of a new ordered vacancy crystal structure in the compound Cu₃In₇Te₁₂, *Rev. Mater.* **24** (2019) e12329, <https://doi.org/10.1590/s1517-707620190001.0643>.
37. G. E. Delgado, C. Rincón, and G. Marroquín, On the crystal structure of the ordered vacancy compound Cu₃In₅□Te₉, *Rev. Mex. Fis.* **65** (2019) 360, <https://doi.org/10.31349/RevMexFis.65.360>.